

## 1. Introduction

Owing to a combination of high strength and toughness Fe–Ni–Co–Mo type maraging steels are being used for many critical applications such as aerospace and military [1]. The material is available in different strength ranges and designated as M250, M350, where 'M' stands for maraging steel, 250 and 350 for their yield strength in ksi. Addition of Ni to Fe- system is responsible for thermal hysteresis gap between the formation of martensite on cooling and its reversion to austenite on heating. This hysteresis allowed material scientists to age the material at peak aged condition to achieve optimum properties with moderate level of fracture toughness with martensitic matrix. Increasing the nickel in this system reduces the austenite ( $\gamma$ )  $\rightarrow$  martensite transformation temperature and it is established that 18% Ni is sufficient to suppress the transformation at RT without rapid cooling from the  $\gamma$ -phase.

Titanium is used as the primary strengthening element and material achieves its strength by precipitation of fine Ti-bearing intermetallic phases dispersed uniformly in the martensitic matrix during aging [2]. Although carbon content is very low, maraging steels are highly alloyed with Nickel, Cobalt, Molybdenum and derive their strength from age hardening of a low carbon, iron, nickel lath martensite. These precipitation hardened Fe–Ni martensitic alloys with very low carbon content meets requirement for fabrication of large sized propellant tanks, bands, tension bolts & studs for space applications [3]. In one such application, maraging steel fasteners (M30X2X90L) were used in nozzle assembly of a satellite launch vehicle.

The fasteners were used in nozzle assembly during one of the static tests and as such they were under sustained load for a period of 2 months under saline humid atmosphere. Further these fasteners were brought in use for some other application, where these fasteners were first given torque to the stress of 180 MPa and were in assembled condition for a period of more than 40 days. When it was further torque to a stress level of 330 MPa, few fasteners sheared off at head-shank junction during torque application. This is to be noted here that these bolts have been used earlier in nozzle assembly during one of the static tests and during that time, they were under sustained load assembly for a period of more than 2 months.

The failed fasteners were subjected to detailed metallurgical investigation to understand the cause for failure. This paper brings out the details of investigation carried out.

## 2. Material

The material used for the fabrication of fasteners was processed through Vacuum Induction Melting (VIM) followed by Vacuum Arc Remelting (VAR). The ingot break down and further hot working was carried out to get rods of 30 mm diameter. The material in solution treated condition (820 °C–1 h–AC) was used for head forming and threads were made through

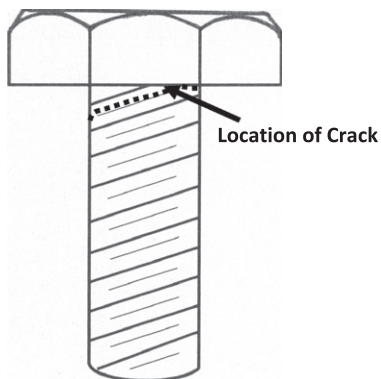


**Fig. 1.** Schematic of fastener showing location of crack.

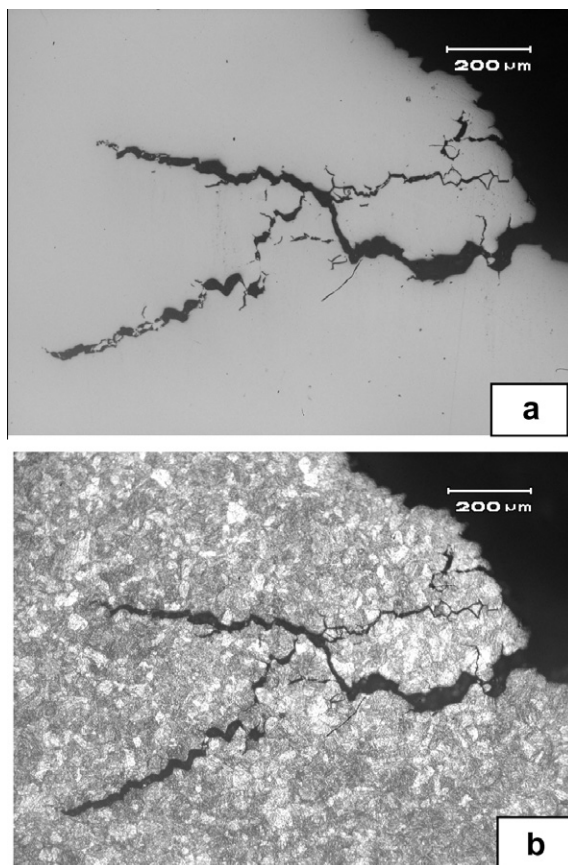


**Fig. 2.** Optical microphotographs showing secondary cracks from primary fracture edge (a) unetched and (b) etched.

thread rolling. The threaded fasteners were aged to 480 °C–3 h–AC to achieve the desired properties. The chemical composition of the alloy in weight percentage was 18.2Ni–4.6Mo–0.42Ti–0.15Al–0.005C–0.02Si–0.022Mn–S&P < 0.005 and balance Fe. Hydrogen was kept low (1 ppm), while oxygen and nitrogen were 15 and 9 ppm respectively. The nominal mechanical properties are YS: min 1725 MPa, UTS: min 1765 MPa, %E on 25 mm, GL: min 8, %RA: min 40 and  $K_{IC}$ : min 90 MPa $\sqrt{m}$ .

### 3. Observations

The location of failure in each one of the three failed fasteners was at head-shank junction. Fig. 1 shows the schematic sketch of fastener and location of crack. Evidence of corrosion was seen at and near the fracture edge. Fracture surface had two distinct regions. One all along the periphery had dark and dull, while the region concentric to centre and irregular in shape was bright in appearance. The parts of failed fasteners were cleaned thoroughly using methanol through ultrasonic means. Threaded region near the fracture edge, under optical microscope with stereographic facility revealed a number of cracks at thread root, very near to the fracture edge. The shank portion was cut across its axis and prepared for optical microscopic observations. Fracture path all along the fracture edge was zig-zag and had a number of secondary cracks with branching along grain boundaries, penetrating into the material (Fig. 2). The crack branching resembled feature of tree root morphology. This was further confirmed when specimens were etched with 3%Nital. Features were indicative of anodic dissolution and even at few locations, grains were detached from the matrix. Thread roots nearby fracture edge too had crack initiation at thread root and their penetration with branching (Fig. 3), typical of tree root morphology.

Fracture surface of failed bolt had two distinct regions. Within outer periphery of the fracture surface, multiple secondary cracks penetrating almost perpendicular to the fracture plane were seen (Fig. 4). It was confirmed that crack initiated at and coincided with region of multiple crack at thread root. Fracture surface at the initiation site had predominantly intergranular mode of fracture with presence of secondary cracks (Fig. 5).

The facets on either side of these grain separation had pits resulted due to local preferential corrosion. at certain locations, grain facets had corrosion product left behind crack advancement (Fig. 6). Central part of the fracture surface had predominantly dimple mode of failure (Fig. 7).

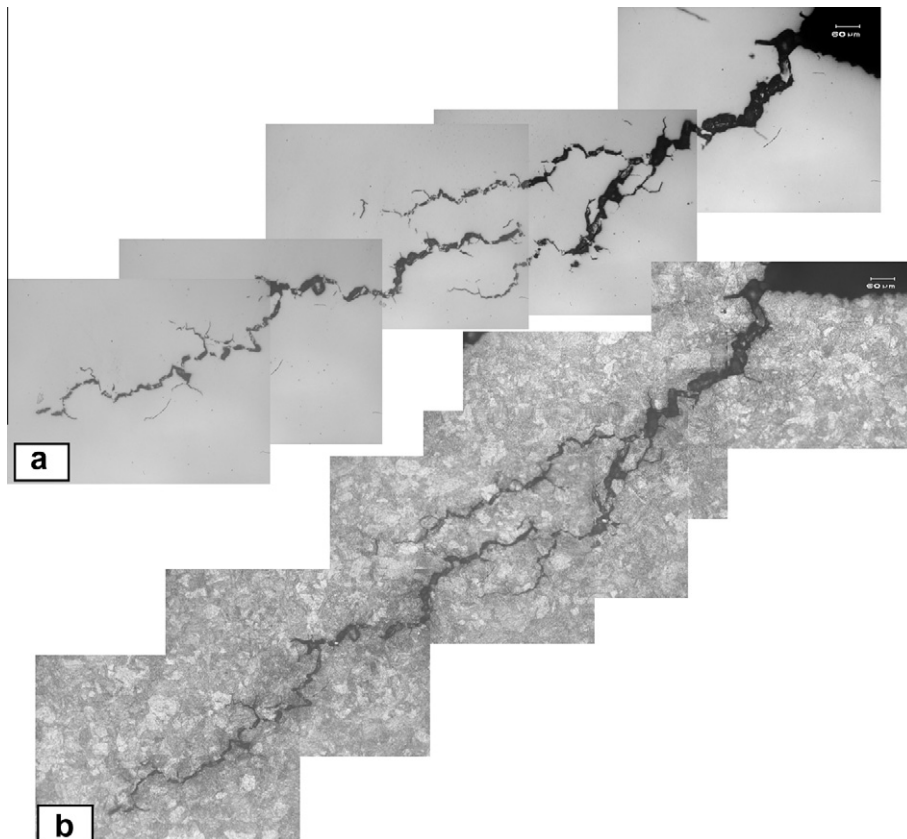


**Fig. 3.** Optical microphotographs showing the crack branching from the thread root near the fracture edge (a) unetched and (b) etched.

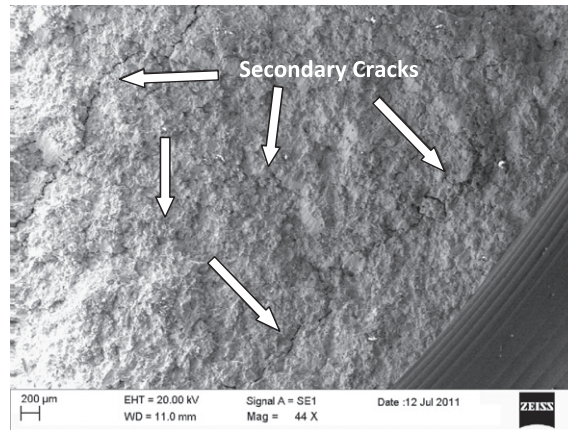


**Fig. 4.** Fractograph showing multiple secondary cracks within outer periphery of the fracture surface.

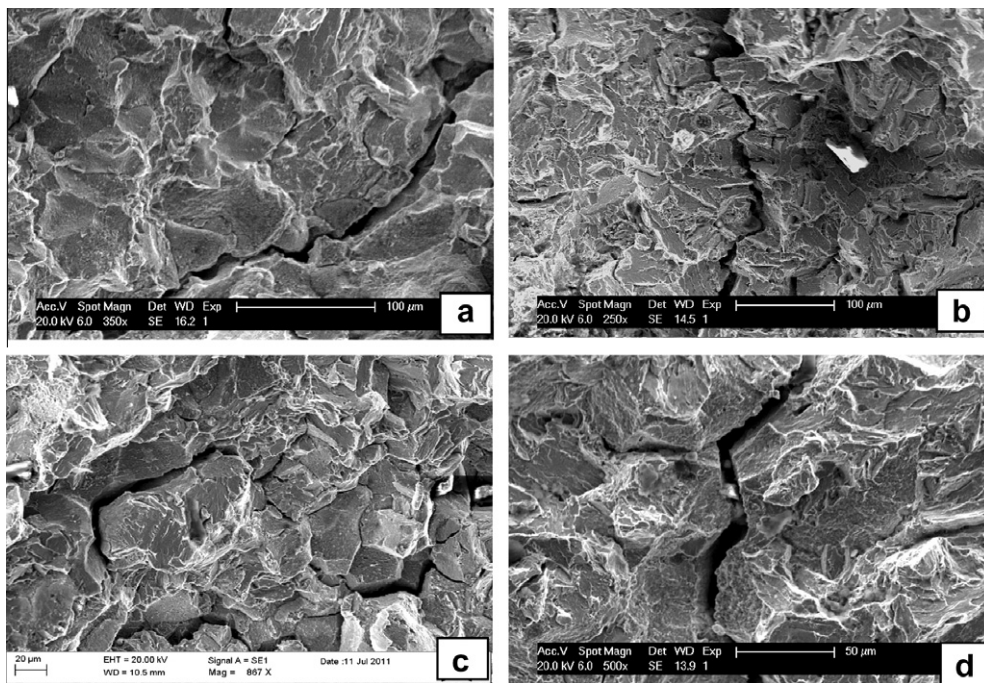


**Fig. 5.** SEM fractographs showing presence of secondary cracks on fracture surface running along the grain boundaries.

#### 4. Discussion

The fasteners were used in nozzle assembly during one of the static tests and as such they were under sustained load for a period of 2 months under humid saline environment. Further these fasteners were used in some other application, where they were in assembled condition under a assembly stress of 180 MPa and when during further torque, stress was raised to 330 MPa, they parted in two. All these indicated this as case of delayed cracking. The intergranular mode of fracture with presence of multiple secondary cracks, evidence of anodic dissolution as evidenced by corrosion product at grain facets indicated failure under synergistic effect of stress (assembly) and corrosion.

It is well established fact that stress corrosion cracking (SCC) resistance of high strength steels in many corrosive media decreases as strength increases. A yield strength of about 1400 MPa and above are vulnerable to catastrophic cracking in corrosive media [4]. The maraging steel grade 18Ni1700 MPa, in solution treated condition with yield strength 1000 MPa showed little or no susceptibility to SCC in 3.5% NaCl solution. The same steel in aged condition with a yield strength of 1700 MPa showed strong susceptibility to SCC [5]. Sastry et al. [6] demonstrated that fracture toughness  $K_Q$  and threshold



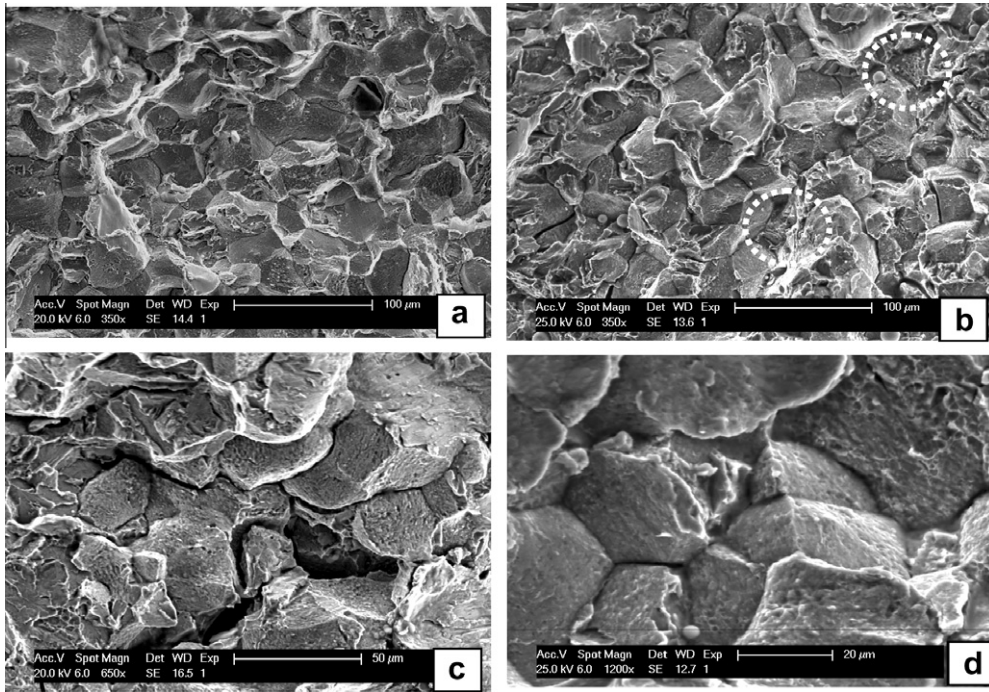


**Fig. 6.** SEM fractographs showing (a) intergranular features, (b) corrosion products and (c and d) pitted facets.

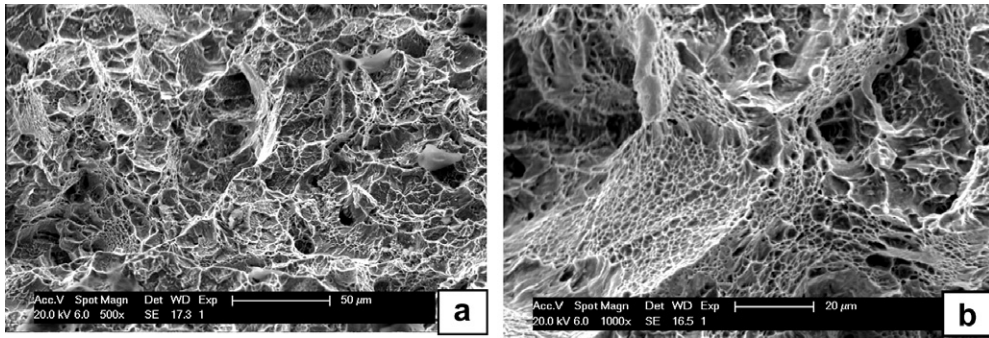


**Fig. 7.** SEM fractographs showing dimple mode of failure within central region of fracture surface.

stress corrosion fracture toughness  $K_{ISCC}$  of the solution treated annealed maraging steel were similar, whereas aging of maraging steel at 480 °C reduced  $K_{ISCC}$  values drastically, as compared to their respective  $K_{ISCC}$  values in an aged condition. The study done by Diwakar et al. [7] indicated that value of critical stress intensity factor  $K_{IC}$  in water came down to the level as low as 8 MPa-m<sup>1/2</sup>. Considering a  $K_{IC}$  value of 10 MPa-m<sup>1/2</sup> for M250 maraging steel, a crack size of even 0.2 mm could not be tolerated for operating stress levels.

The SCC of maraging steel band used for a satellite launch vehicle has been studied by Jha et al. [8], who established that the cracking was intergranular in nature. Stavros and Paxton [9] as well as Rao et al. [10] carried out extensive study on SCC behavior of maraging steel and the crack path was established to be intergranular. Brook and Muciol [11] also established that the environmental susceptibility was associated with a corrosive susceptible path.

In the present case study, the fastener experienced sustained load and exposed to saline atmosphere of marine coast for a period of 2 months. Further they were in assembly under torque of 50 Kgf-m for 40 days. Cracks at thread roots next to fracture edge and their penetration into the core of material confirmed that simultaneously cracks were active at roots of more than one thread. The corrosion product at crack tip and morphology suggested role of corrosion during crack propagation. Fracture surface had predominantly intergranular mode of fracture, a typical feature of stress corrosion cracking of maraging steel.

Taking considerations of evidences collected from failed fasteners and above discussions, following points converged as conclusive out come.

1. There was corrosion within the engaged threads, which caused cracks to initiate at thread roots and propagated under influence of load (assembly).
2. Crack propagation was intergranular.
3. Corrosion products at crack tip as well as within grain separation gap were conclusive evidence of anodic dissolution during crack advancement.